



Compressibility effects on the dynamic characteristics of gas lubricated mechanical components

Mihai Arghir*, Pierre Matta

Laboratoire de mécanique des solides, université de Poitiers, 86962 Futuroscope Chasseneuil, France

Received 10 June 2009; accepted after revision 31 August 2009

Available online 7 October 2009

Presented by Jean-Baptiste Leblond

Abstract

The present Note deals with the effects of compressibility on the linearized dynamic characteristics of gas lubricated mechanical components (journal and thrust bearings). Although the effect of compressibility on the *static* characteristics is well known, its influence on the *dynamic* characteristics is still not clearly understood. The present Note uses Lubrication's simplest model problems (the 1D slider) to qualitatively describe this effect. An analytic solution obtained for the parallel 1D slider depicts the variation of stiffness and damping with the excitation frequency and shows that this nonlinearity must be taken into account for squeeze number larger than 1. A convenient way of handling this nonlinearity in a dynamic system is described for an aerodynamic thrust bearing. **To cite this article:** *M. Arghir, P. Matta, C. R. Mecanique 337 (2009).*

© 2009 Académie des sciences. Published by Elsevier Masson SAS. All rights reserved.

Résumé

Effets de la compressibilité sur les caractéristiques dynamiques des composants mécaniques lubrifiés avec des gaz. L'article présente les effets de la compressibilité sur les caractéristiques dynamiques linéaires des composants mécaniques lubrifiés avec des gaz (paliers et butées). Même si les effets de la compressibilité sur les caractéristiques statiques sont bien connus, son influence sur les caractéristiques dynamiques n'est pas encore clairement soulignée. L'article utilise le modèle le plus simple de la lubrification (le blochet 1D) pour décrire qualitativement cet effet. Une solution analytique développée pour le blochet 1D à faces parallèles décrit la variation de la raideur et de l'amortissement avec la fréquence d'excitation et montre que cette nonlinéarité doit être prise en compte pour des nombres d'écrasement supérieurs à 1. Une voie possible de traiter cette nonlinéarité dans un système dynamique est exemplifiée pour une butée aérodynamique. **Pour citer cet article :** *M. Arghir, P. Matta, C. R. Mecanique 337 (2009).*

© 2009 Académie des sciences. Published by Elsevier Masson SAS. All rights reserved.

Keywords: Lubrication; Gas lubrication

Mots-clés : Lubrification ; Lubrification avec gaz

* Corresponding author.

E-mail address: Mihai.Arghir@lms.univ-poitiers.fr (M. Arghir).

Nomenclature

| | | | |
|-----------------|---|---------------------|---|
| A_0, A_1, B_0 | parameters of the transfer function | V | linear velocity m/s |
| B_1, B | slider width m | W | load N |
| C | damping Ns/m | β_1, β | thrust bearing pad angular amplitude |
| F | force N | Λ | compressibility number |
| H | transfer function | σ | squeeze number |
| h | thin film thickness m | Ω | thrust bearing rotation speed 1/s |
| K | stiffness N/m | ω | squeeze angular velocity 1/s |
| L | length m | ω_0 | natural speed 1/s |
| M | mass kg | μ | dynamic viscosity Pa s |
| N_p | number of pads of the thrust bearing | ζ | damping ratio |
| P | pressure averaged over the thin film | ν | volume m ³ |
| | thickness Pa | Δ | small perturbation |
| P_a | atmospheric pressure Pa | 1D, 2D | one/two dimensional |
| $R_{1,2}$ | thrust bearing inner/outer radius m | <i>Superscripts</i> | |
| r, θ, z | cylindrical coordinate system | \sim | complex number |
| \Re | real part | \cdot | time derivative |
| S | thrust bearing surface, $\pi(R_2^2 - R_1^2)$. . . m ² | | |
| t | time s | | |

1. Introduction

Gas lubrication theory is based on the same simplifying assumptions as the incompressible lubrication [1], all stemming from the presence of two very different length scales H and R (or L) of the order $H/R \approx 10^{-3}$: negligible inertia and body forces, constant pressure over the thin film thickness, isothermal and laminar flow (the last two assumptions can easily be relaxed). For comparison, the ratio of the two length scales intervening in the boundary layer theory is 10^{-2} and the convective inertia forces are not negligible. Lubrication theory is generally (but not exhaustively) applied for the study of journal and thrust bearings or for dynamic sealing systems. Although it is a very mature domain disposing of specific modeling tools, such as the Reynolds equation, some aspects can pose interpretation problems and need to be underlined. The compressibility of the thin lubricant film is such of an aspect. Its influence on the static characteristics (load capacity) is well known but the way it affects the dynamic stiffness and damping (characteristics needed for describing the vibration regime) is not clearly quantified. The aim of the present work is to underline the influence of the gas compressibility on the dynamic characteristics and to convey a simple solution of including them in a vibration model. This is done by using a usual gas (air) in conjunction with a model problem (the 1D slider) and a simple mechanical component (the thrust bearing) where the compressible Lubrication theory is applied.

2. The 1D slider

The main peculiarities brought in by the compressibility of the air film can be best explained by analysing first a 1D slider of infinite width as the one depicted in Fig. 1 (step or ‘‘Rayleigh slider’’). The 1D slider is the simplest problem analyzed in the Lubrication theory and the source of basic lifting mechanisms. It is supposed that the two plates are closely spaced so that $h_{1,2}/B$, $B_1 \approx 10^{-3}$ and the lower one has a horizontal velocity V . The appropriate dimensionless Reynolds equation yields:

$$\frac{\partial}{\partial \bar{x}} \left(\bar{P} \bar{h}^3 \frac{\partial \bar{P}}{\partial \bar{x}} \right) = \Lambda \frac{\partial}{\partial \bar{x}} (\bar{P} \bar{h}) + \sigma \frac{\partial}{\partial \bar{t}} (\bar{P} \bar{h}), \quad \Lambda = \frac{6\mu V B}{P_a h_2^2}, \quad \sigma = \frac{12\mu \omega B^2}{P_a h_2^2} \quad (1)$$

$$\bar{x} = x/B, \quad \bar{P} = P/P_a, \quad \bar{h} = h/h_2, \quad \bar{t} = \omega t \quad (2)$$

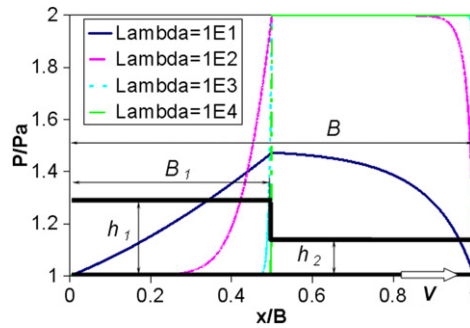


Fig. 1. Static pressure variation of the 1D step slider.

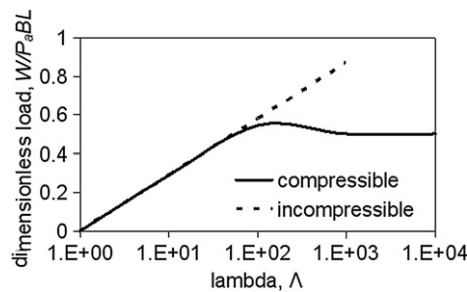


Fig. 2. Static load of the 1D step slider.

This equation is solved with imposed (atmospheric) pressure boundary conditions at its left and right ends. Fig. 1 depicts the pressure variation for different compressibility numbers and steady working conditions, i.e. $\sigma = \omega = 0$. Fig. 2 depicts the corresponding static load obtained by integrating the pressure field. The solution depends not only on x/B , h_1/h_2 and B_1/B as for an incompressible fluid, but the compressibility number Λ has now a strong influence. For $\Lambda \rightarrow 0$ the pressure variation corresponds to the incompressible solution while for high Λ the pressure tends toward an asymptotic solution. Fig. 2 shows that with increasing Λ the dimensionless load capacity of the compressible slider tends toward a constant value while for an incompressible lubricant it increases linearly with the sliding velocity. This typical result for compressible lubrication stems from the fact that the right-hand side of the steady Reynolds equation $\Lambda \partial(\bar{P}\bar{h})/\partial\bar{x}$ must have a finite value for high Λ . It then results that $Ph = const.$ for $\Lambda \rightarrow \infty$. The result is coherent with the assumption of an isothermal evolution of the gas because it can be alternatively written as $P d\vartheta = P/\rho = const.$ where $d\vartheta = h dx L$ is the fluid volume for the 1D slider of length L .

This well-known result reflects a fundamental characteristic of compressible lubrication that can be found also for the unsteady (vibration) regime engendered by a squeeze motion of the plates. In order to enable an analytic solution for the compressible unsteady squeeze regime, the 1D slider can be simplified even more by considering only two infinitely long parallel plates of width B . The pressure between the two plates is generated by the oscillatory squeeze motion of the upper plate. The Reynolds equation yields:

$$h^3 \frac{\partial^2 P^2}{\partial x^2} = 24\mu \frac{\partial}{\partial t}(Ph) \tag{3}$$

with boundary conditions, $x = 0, \partial P/\partial x = 0$ and $x = \pm B/2, P = P_a$. An analytic solution is obtained under the assumption of a low amplitude squeeze oscillatory motion of the upper plate:

$$h(t) = h_0 + \Delta h(t) \tag{4}$$

$$\Delta h(t) = \Re(\Delta \tilde{h} e^{j\omega t}), \quad j = \sqrt{-1}, \quad |\Delta \tilde{h}| \ll h_0 \tag{5}$$

It is supposed that the pressure has a similar variation [2]:

$$P(t) = P_a + \Delta P(x, t) \tag{6}$$

$$\Delta P(x, t) = \Re[\Delta \tilde{P}(x) e^{j\omega t}], \quad j = \sqrt{-1}, \quad |\Delta \tilde{P}(x)| \ll P_a \tag{7}$$

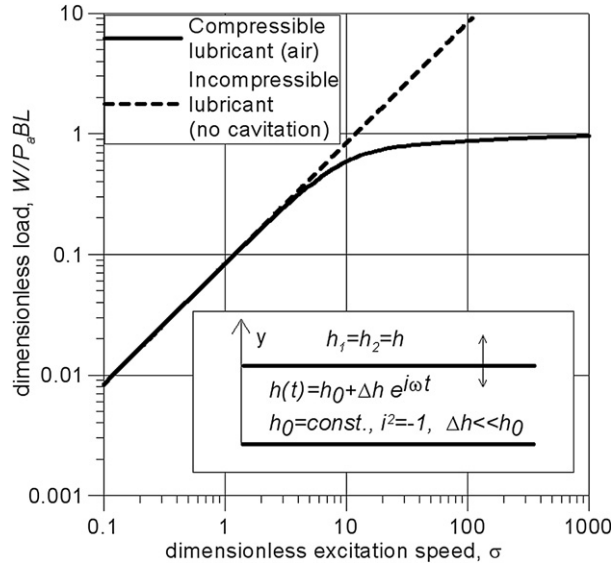


Fig. 3. Dynamic load capacity of the 1D parallel slider.

where it was recognized that if the oscillatory squeeze motion is absent, $\omega = 0$ then the zeroth order pressure is $P_0 = P_a$. Following the small perturbation assumption¹

$$h^3 P^2 = (h_0^3 + 3h_0^2 \Delta h e^{j\omega t} + \dots)(P_a^2 + 2P_a \Delta P e^{j\omega t} + \dots) \approx h_0^3 P_a^2 + 2h_0^3 P_a \Delta P e^{j\omega t} + 3h_0^2 P_a^2 \Delta h e^{j\omega t} \quad (8)$$

$$h P \approx h_0 P_a + h_0 \Delta P e^{j\omega t} + P_a \Delta h e^{j\omega t} \quad (9)$$

the Reynolds equation yields:

$$\frac{\partial^2(\Delta P)}{\partial x^2} = \frac{12\mu j\omega}{P_a h_0^2} \Delta P + \frac{12\mu j\omega}{h_0^3} \Delta h \quad (10)$$

with boundary conditions, $x = 0, \partial(\Delta P)/\partial x = 0$ and $x = \pm B/2, \Delta P = 0$. The analytic solution of this differential equation is:

$$\frac{\Delta P}{P_a} = \frac{\Delta h}{h_0} \left[\frac{\text{ch}(\sqrt{\sigma} e^{j\pi/4} x/B)}{\text{ch}(\sqrt{\sigma} e^{j\pi/4} /2)} - 1 \right], \quad \sigma = \frac{12\mu\omega B^2}{P_a h_0^2} \quad (11)$$

The dynamic load is obtained by integrating the first order pressure field.

$$\Delta F = 2L \int_0^{B/2} (P - P_a) dx = \Delta \tilde{F} e^{j\omega t}, \quad \Delta \tilde{F} = LBP_a \frac{\Delta \tilde{h}}{h_0} \left[2 \frac{\text{th}(\sqrt{\sigma} e^{j\pi/4} /2)}{\sqrt{\sigma} e^{j\pi/4}} - 1 \right] \quad (12)$$

The modulus of the dimensionless dynamic load, $|\Delta \tilde{F}|/LBP_a$ is depicted in Fig. 3. Also depicted on Fig. 3 is the modulus of the dimensionless load for the incompressible parallel slider obtained under the small perturbation assumption²:

$$\Delta \tilde{F}^{incomp} = LBP_a \frac{\sigma}{12} \frac{\Delta \tilde{h}_1}{h_0} e^{-j\pi/2} \quad (13)$$

¹ For simplifying equations, superscript \sim and operator \Re were dropped.
² Relation (13) was obtained by discarding the cavitation phenomenon and film rupture that occurs in incompressible lubrication for pressures slightly below P_a .

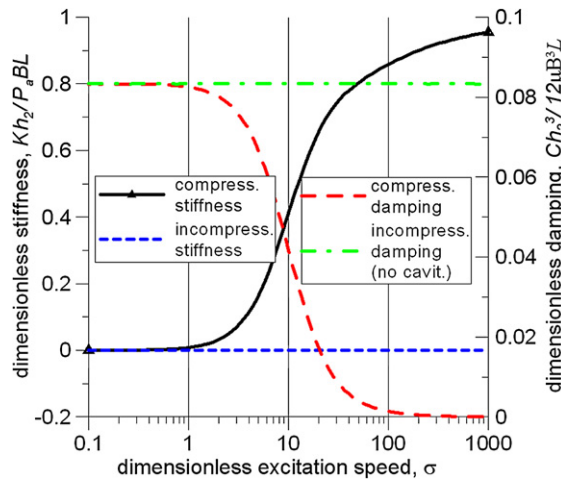


Fig. 4. Dynamic coefficients of the 1D parallel slider.

Fig. 3 shows that the modulus of the dynamic load given by (12) tends to a constant value with increasing excitation speed while the dynamic load of the incompressible parallel slider is linearly increasing. This is exactly the same characteristic as the one depicted in Fig. 2 for the static load excepting the fact that the parameter Λ is replaced by σ .

The consequences on the dynamic stiffness and damping (linearized) coefficients can be also underlined from the analytic solution (12). These coefficients can be identified from the following definition:

$$\Delta F = K \Delta h + C \Delta \dot{h} = (K \Delta \tilde{h}_1 + j \omega C \Delta \tilde{h}_1) e^{j \omega t} \tag{14}$$

One obtains:

$$\bar{K} = \frac{K h_0}{L B P_a} = \Re \left[2 \frac{\text{th}(\sqrt{\sigma} e^{j \pi/4} / 2)}{\sqrt{\sigma} e^{j \pi/4}} - 1 \right] \tag{15}$$

$$\bar{C} = \frac{C h_0 \omega}{L B P_a} = \Im \left[2 \frac{\text{th}(\sqrt{\sigma} e^{j \pi/4} / 2)}{\sqrt{\sigma} e^{j \pi/4}} - 1 \right] \tag{16}$$

The dimensionless dynamic stiffness and damping coefficients are depicted in Fig. 4. The dynamic coefficients stemming from the incompressible slider are both constant (the stiffness is zero while the damping has a nonzero value) while the ones obtained for the compressible slider vary with the excitation frequency. As shown in Fig. 4, for $\sigma \rightarrow 0$ the compressible and the incompressible coefficients tend to the same values but starting with $\sigma > 1$ the dynamic coefficients of the compressible slider depend on the excitation frequency. For increasing excitation frequency the dynamic stiffness of the compressible slider increases while the damping coefficient decreases toward zero. This means that with increasing excitation frequency the compressible slider becomes stiffer and has a negligible damping. This is a general characteristic of aerodynamic lubrication that will influence the dynamic properties of thrust and journal bearings.

3. The 2D thrust bearings

The compressibility influence on the dynamic characteristics is illustrated for one of the most simple gas lubricated mechanical components. Thrust bearings as the one depicted in Fig. 5 are aimed to support an axial load or to eliminate the axial degree of freedom of a rotor guided by aerodynamic bearings. The flow field comprised between the runner (upper part rotating with Ω) and the stepped thrust bearing is 2D because the pressure is considered as being constant over the thin film thickness.

The gas flow in the thrust bearing is governed by the compressible Reynolds equation in cylindrical coordinates; in dimensionless form this equation yields:

$$\frac{1}{\bar{r}} \frac{\partial}{\partial \bar{r}} \left(\bar{p} \bar{h}^3 \bar{r} \frac{\partial \bar{p}}{\partial \bar{r}} \right) + \frac{\partial}{\partial \bar{r}} \left(\bar{p} \bar{h}^3 \frac{\partial \bar{p}}{\partial \theta} \right) = \Lambda \frac{\partial(\bar{p} \bar{h})}{\partial \theta} + \sigma \frac{\partial(\bar{p} \bar{h})}{\partial \bar{t}} \tag{17}$$

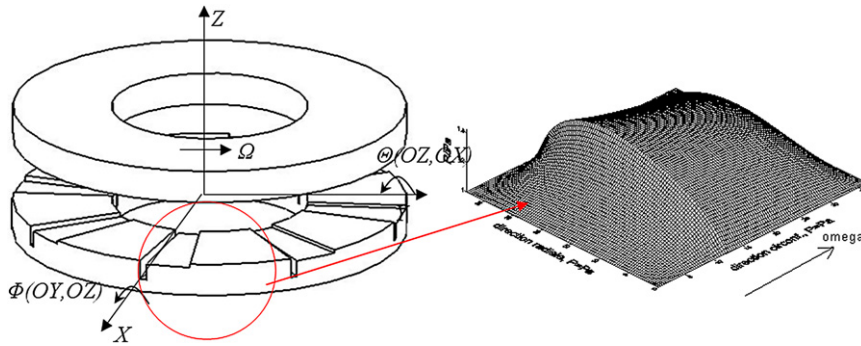


Fig. 5. Thrust bearing geometry and typical pressure field.

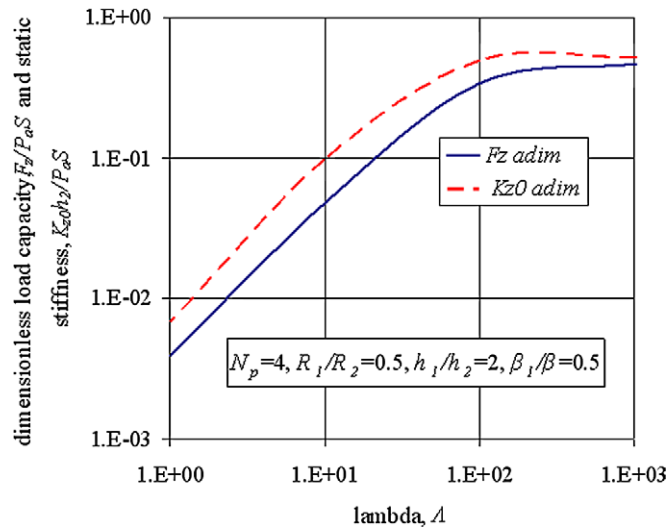


Fig. 6. Static characteristics of the thrust bearing.

The boundary conditions are represented by an imposed (atmospheric) pressure on the inner and outer radius as well as in the feeding grooves separating the thrust bearing pads. The numerical solution of the 2D compressible Reynolds equation can be obtained by using a finite volume algorithm that will not be presented for brevity. Fig. 6 depicts the dimensionless axial load capacity and the torque of the thrust bearing. As for the compressible 1D slider the dimensionless axial load tends toward a constant value with increasing rotation speed and Λ .

The dynamic characteristics of the thrust bearing are obtained by following the small perturbation approach presented for the 1D slider and given by Eqs. (4)–(9). For example for an axial Z displacement the thin film thickness and the pressure perturbations are injected into Eq. (17) yielding a first order compressible Reynolds equation. The perturbed (first order) pressure field is obtained after numerically solving this equation with $\Delta \tilde{P} = 0$ overall boundary conditions. The dynamic stiffness and damping (linearized) coefficients are calculated by integrating $\Delta \tilde{P}$ over the thrust bearing surface.

$$\Delta F = \int_S \Delta \tilde{P} dS = K_Z \Delta h + C_Z \Delta \dot{h} \tag{18}$$

As for the 1D parallel slider, the dynamic coefficients of the thrust bearing depend not only on the working conditions but also on the excitation frequency (Fig. 7). This nonlinear dependence of the dynamic coefficients K_Z and C_Z on the excitation frequency must be carefully considered in any dynamic analysis of a mechanical system incorporating a compressible thin film. For example if the thrust bearing supports a mass M , the equation of the 1DOF oscillator yields:

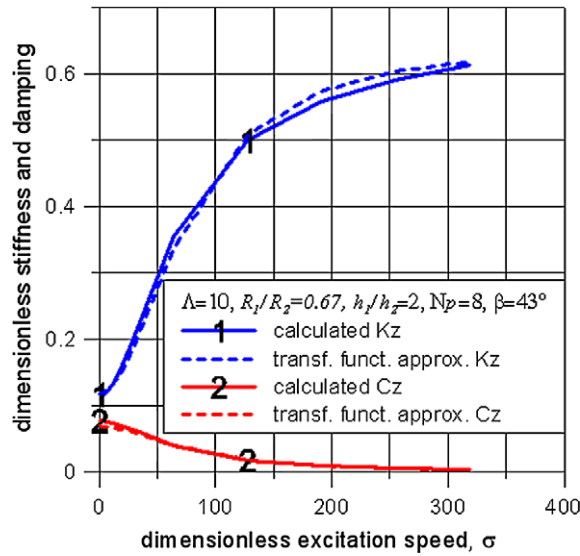


Fig. 7. Dynamic coefficients of the thrust bearing.

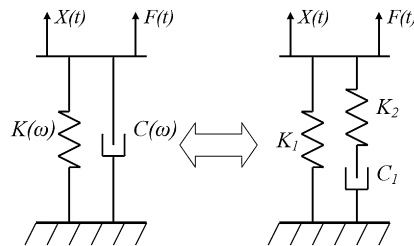


Fig. 8. Viscoelastic model of the squeezed gas film.

$$M\Delta\ddot{z} + \underbrace{C_Z\Delta\dot{z} + K_Z\Delta z}_{\Delta F_z} = \Delta W(t) \tag{19}$$

This equation is nonlinear because K_Z and C_Z depend on the perturbation squeeze velocity \dot{z} . There are two possible solutions. The first is to use the step jump method based on Duhamel’s integral [3]. The second method is more appropriate because it offers a better insight into the thrust bearing dynamics by using less parameter. The idea stems from recognizing that the compressible thin film of a perfect gas behaves as a viscoelastic material when subject to squeeze [4] & [5]. The usual practice for viscoelastic materials is to replace the usual model made of a linear spring and a viscous damper by a slightly modified one as depicted in Fig. 8. The transfer function of the viscoelastic model yields:

$$H(s) = \frac{\Delta z(s)}{\Delta F(s)} = \frac{B_0 + s}{A_0 + sA_1} \tag{20}$$

where s is the variable of the Laplace transform. If one takes into account the equivalence between Laplace transform and Fourier transform for a sinusoidal excitation, $s = j\omega$ one obtains:

$$\frac{\Delta \tilde{F}(\omega)}{\Delta \tilde{z}(\omega)} = K_Z + j\omega C_Z = \frac{A_0 + j\omega A_1}{B_0 + j\omega} \tag{21}$$

It then follows that the variable K_Z and C_Z can be expressed by using only three constants, A_0 , A_1 and B_0 .³ Their identification is straightforward by minimizing the nonlinear function:

³ Second order transfer function can be used for enhancing the nonlinear dependence of the dynamic coefficients on the excitation frequency.

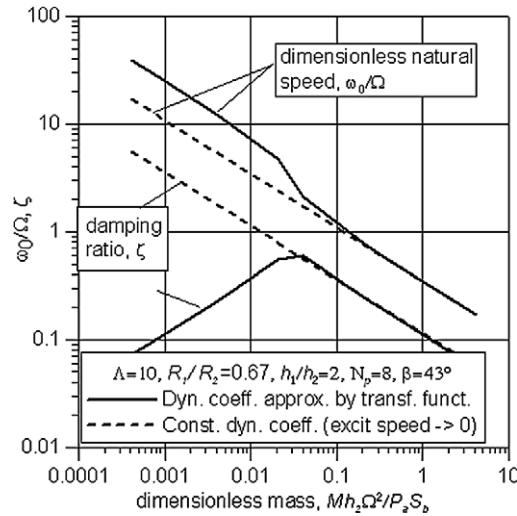


Fig. 9. Unforced response dynamic characteristics of the thrust bearing—mass system.

$$\text{Minimizer } \sum_i \left(K_Z + j\omega_i C_Z - \frac{A_0 + j\omega_i A_1}{B_0 + j\omega} \right) \tag{22}$$

$$K_Z(\omega) = \frac{A_0 B_0 + \omega^2 A_1}{B_0^2 - \omega^2}, \quad C_Z(\omega) = \frac{A_1 B_0 - A_0}{B_0^2 - \omega^2} \tag{23}$$

An example of this approach is depicted in Fig. 7. It is to be underlined that these transfer functions are only approximations of the complex impedance based on rational functions. Together with the minimization procedure of Eq. (22) they simply provide a nonlinear regression. A similar procedure was used by Kleyhans and Childs [6] for textured annular gas seals and the viscoelastic model depicted in Fig. 8 was also advocated by Brad and Green [7]. Also, an analytic demonstration of first order transfer functions was introduced in [8] and was next used in [9] & [10] for modeling the dynamic behavior of a circular *aerostatic* thrust bearing.

The benefits of using this transfer function approach can be best understood when analysing the 1DOF oscillator. The equation of its dynamic system is obtained by considering Eqs. (19) and (20):

$$\begin{Bmatrix} \Delta \dot{z} \\ \Delta \ddot{z} \\ \Delta \dot{F}_z \end{Bmatrix} = \begin{bmatrix} 0 & 1 & 0 \\ 0 & 0 & -1/M \\ A_0 & A_1 & -B_0 \end{bmatrix} \begin{Bmatrix} \Delta z \\ \Delta \dot{z} \\ \Delta F_z \end{Bmatrix} + \begin{Bmatrix} 0 \\ \Delta W(t)/M \\ 0 \end{Bmatrix} \tag{24}$$

Classical problems as the unforced response or the response to an impact load can be easily answered. Fig. 9 depicts the natural speed and the damping ratio of the unforced response of the thrust bearing—mass system. The parameters intervening in the characteristic equation $r^2 + 2\zeta\omega_0 r + \omega_0^2 = 0$ of the 1DOF damped system made of the thrust bearing and the mass M . The natural speed ω_0 and the damping ratio are calculated for different values of the mass M by using two approaches:

1. by considering the eigenvalues of the matrix given in Eq. (24), i.e. by taking into account the fact that the dynamic coefficients depend on the excitation frequency,
2. by considering the values of the dynamic coefficients obtained for a very low value of the excitation frequency.

It can be seen that errors are unacceptable if the variation of the dynamic coefficients with the excitation frequency is discarded: for values of the dimensionless mass lower than 0.1, the natural speed is underestimated and the damping ratio is largely overestimated. In fact, the system might appear as being overdamped if constant dynamic coefficients are used while in reality the damping coefficient decreases with decreasing the dimensionless mass.

4. Conclusion

The presented results underline the importance of taking into account the dependence of dynamic coefficients of a compressible thin film on the excitation frequency. As shown by using a very simple 1D example, this should be done for $\sigma > 1$ because the squeeze parameter σ plays the same role as the compressibility number Λ . The analytic results for the 1D compressible squeeze flow are hereby presented for the first time. As a further example, the frequency dependence of dynamic coefficients was depicted for a thrust bearing but the effect can be retraced for any mechanical component lubricated by compressible thin film (journal bearing, dynamic seal, etc.).

References

- [1] J. Frêne, D. Nicolas, B. Deguerce, D. Berthe, M. Gaudet, *Lubrification hydrodynamique. Paliers et Butées*, Editions Eyrolles, 1990, 488 pp.
- [2] J.W. Lund, Calculation of stiffness and damping properties of gas bearings, *ASME Journal of Lubrication Technology* 90 (4) (1968) 793–803.
- [3] H.G. Elrod, J.T. McCabe, T.Y. Chu, Determination of gas-bearing stability by response to a step-jump, *ASME Journal of Lubrication Technology* (1967) 493–498.
- [4] R.M.J. Liebrechts, *Rotordynamics of a grindle spindle supported with airbearings*, Nat. Lab. Technical Note No. 259/88, Philips NatLab Confidential Report, 1988 (in Dutch).
- [5] N. Geerts, *Linear dynamic analysis of rotorsystems with gas bearings*, Master's thesis, Eindhoven University of Technology, September 1995.
- [6] G. Kleynhans, D. Childs, The acoustic influence of cell depth on the rotordynamic coefficients of smooth-rotor/honeycomb-stator annular seals, *ASME Journal of Engineering for Gas Turbines and Power* 119 (1997) 949–957.
- [7] B. Miller, Y. Green, On the stability of gas lubricated triboelements using the step jump method, *ASME Journal of Tribology* 119 (1) (1997) 193–199.
- [8] J.W. Roblee, *Design of externally pressurized gas bearings for dynamic applications*, PhD thesis, University of California, Berkeley, CA, 1985.
- [9] M. Fourka, *Modélisation par la méthode des éléments finis des paliers à gaz en régime aérostatique et hybride*, Thèse de Doctorat, Université de Compiègne, Compiègne, 1994.
- [10] M. Fourka, Y. Tian, M. Bonis, Prediction of the stability of air thrust bearings by numerical, analytical and experimental methods, *Wear* 198 (1998) 1–6.